scientific reports

Check for updates

OPEN

Green synthesis of silver nanoparticles from *Eichhornia crassipes* and evaluates their antimicrobial properties against multidrug-resistant UTI pathogens

Imdadul Haque Sharif[1], Farjana Sultana Primu[1], Md. Nahid Hasan Joy[1], Monika Halder Tithi[1], Ashik Chowdhury[1], Pradipta Debnath Pretha[2], Abu Hena Mostafa Jamal[3], Tusar Kanti Roy[4]✉, Zulhilmi Ismail[5,6]✉, Md. Saiful Islam[6,7]✉ & Abubakr M. Idris[8,9]✉

Multidrug resistance is a rising concern for global public health. Antibiotic and antifungal resistance infections demand new antimicrobial approaches. This is the first time Silver Nanoparticles (Ag NPs) were biosynthesized using *Eichhornia crassipes* leaf extract as a natural reducing and stabilizing agent in Bangladesh. The Ultraviolet–Visible (UV–vis) spectra observed at 468 nm and 454 nm, with a maximum absorbance of 1.516 for the 1:2 ratio (60 min) and 0.546 for the 1:2 ratio (30 min), respectively. Fourier Transform Infrared (FTIR) spectra indicated that functional groups, including 3333.11 cm^{-1} (51.06% T) for carboxyl, 2191.23 cm^{-1} (97.27% T) for alkyne, 1632.58 cm^{-1} 74.89% T) for carbonyl, and 627.08 cm^{-1} (91.6% T) for chlorinated groups in the leaf extract, probably contribute to the reduction of metallic ions and the formation of nanoparticles. The antibacterial effectiveness of the synthesized Ag NPs was evaluated against antibiotic-resistant bacterial strains obtained from patients with Urinary Tract Infections (UTIs) at Kushtia Sadar Hospital, as well as against fungal infections. The disk diffusion technique is used to evaluate the antibacterial and antifungal activity, as well as the Minimum Inhibitory Concentration (MIC) and the Minimum Bactericidal/Fungicidal Concentration (MBC/MFC) tests. Notably, the synthesized Ag NPs exhibited significant antimicrobial activity against MEBTN 4(EF) and MEBTN 6(EF), with inhibition zone diameters ranging from 6 ± 0.1 to 13 ± 0.1 mm. The MIC and MBC values against MEBTN 6(EF) were 15 µg/mL and 60 µg/mL, respectively, indicating strong bactericidal activity. Antifungal assays revealed a MIC value of 18 µg/mL. The findings revealed substantial antimicrobial efficacy of Ag NPs against Multidrug-Resistant (MDR) UTI pathogens and pathogenic fungi, underscoring their broad-spectrum effectiveness in a new era of treatment. Future research should prioritize comprehensive in vivo toxicity assessments, elucidation of the underlying mechanisms, investigation of anti-cancer properties, including ROS-mediated effects, and optimization of large-scale production processes.

Keywords Silver nanoparticle, *Eichhornia crassipes*, Urinary tract infections, Multi-drug resistance, Antibacterial, Green synthesis

[1]Department of Biotechnology and Genetic Engineering, Faculty of Life Science, Gopalganj Science and Technology University, Gopalganj 8100, Bangladesh. [2]Faculty of Veterinary, Animal and Biomedical Sciences, Khulna Agricultural University, Khulna 9202, Bangladesh. [3]Department of Biotechnology and Genetic Engineering, Medical and Environmental Biotechnology Lab, Islamic University, Kushtia 7003, Bangladesh. [4]Department of Agricultural Chemistry, Khulna Agricultural University, Khulna 9202, Bangladesh. [5]Centre for River and Coastal Engineering (CRCE), Universiti Teknologi Malaysia (UTM), 81310 Bahru, Johor, Malaysia. [6]Department of Water and Environmental Engineering, Faculty of Civil Engineering, Universiti Teknologi Malaysia (UTM), 81310 Skudai, Johor, Malaysia. [7]Department of Soil Science, Patuakhali Science and Technology University, Dumki, Patuakhali 8602, Bangladesh. [8]Department of Chemistry, College of Science, King Khalid University, 62529 Abha, Saudi Arabia. [9]Research Center for Advanced Materials Science (RCAMS), King Khalid University, 62529 Abha, Saudi Arabia. ✉email: tusar@kau.ac.bd; zulhilmi@utm.my; msaifulpstu@yahoo.com; dramidris@gmail.com

Nanotechnology is the ability to manipulate materials at the atomic level through engineering techniques of particles that vary in size from 1 to 100 nm[1,2]. Metal nanoparticles possess unique physicochemical properties, including strong optoelectronic and thermal behavior, high catalytic efficiency, and a large surface-to-volume ratio, along with tunable morphology and crystallinity[3].

Silver nanoparticles (Ag NPs) can be synthesized using physical, chemical, or biological approaches. However, physical and chemical methods often involve long preparation times, high costs, elevated temperatures and pressures, substantial energy consumption, and limited environmental sustainability[4,5]. The physical approach, using techniques such as gas-phase deposition, laser ablation, and mechanical grinding, offers simplicity and high purity but generally produces larger nanoparticles than chemical or biological methods[4]. The chemical method uses reducing agents, such as sodium citrate or sodium borohydride, to convert Ag^{+} to Ag^{0} and stabilizing agents to prevent nanoparticle aggregation[5,6]. Synthesized nanomaterials must retain their biocompatibility[7], as chemically synthesized materials can exert adverse effects on both human health and the environment[8–11]. These inherent limitations, therefore, highlight the need to develop alternative methods that are safer for Ag NPs synthesis. Biological techniques mitigate several of these limitations by synthesizing silver nanoparticles via diverse biological agents, including yeasts, enzymes, bacteria, polysaccharides, algae, oligosaccharides, fungi, DNA (Deoxyribonucleic Acid), and human cell lines[12]. Ag NPs are among the most prominent nanomaterials in the field of nanotechnology. At low concentrations, they exhibit minimal toxicity to human health. Ag NPs are widely applied across various sectors, including textiles and apparel, food packaging, medical and cosmetic formulations, water, wastewater, and air treatment systems, as well as in pesticides and general household products.

The use of plant extracts is more advantageous than using microorganisms, owing to reduced costs, since it eliminates the need for specialized culture and isolation procedures, and it can be readily scaled for large-scale nanoparticle synthesis[5,13]. The use of plants and their extracts in the green synthesis of metal nanoparticles is advantageous due to their abundance, non-toxicity, pollution-free, environment-friendly, economical, sustainable, ease of handling, and diverse array of metabolites that may facilitate the reduction process[13]. Green synthesis represents a bottom-up methodology analogous to conventional chemical reduction, but it substitutes costly chemical reducing agents with extracts derived from natural sources such as leaves of various plants, crops, or fruits, to facilitate the formation of metal or metal-oxide nanoparticles[14]. Plant extracts may function as both reducing and stabilizing agents for metal nanoparticles. The process of reduction and stabilization involves the combination of biomolecules, including proteins, amino acids, enzymes, polysaccharides, alkaloids, flavonoids, tannins, phenols, saponins, terpenoids, and vitamins[5]. Nonetheless, the dimensions, morphology, and antibacterial properties of nanoparticles generated through plant sources are influenced by the specific type and concentration of phytochemicals in the plant, the temperature during synthesis, and the duration of the reaction.

The application of plant extracts presents numerous benefits, as the resulting by-products are typically biocompatible, eco-friendly, and exhibit a lower risk of contamination[15,16]. Ag NPs have previously been synthesised using various medicinal plants, including *Artemisia nilagirica, Ocimum sanctum, Catharanthus roseus, Cynodon dactylon, Azadirachta indica, Aegle marmelos, Hibiscus cannabinus, Aloe vera, Zea mays, Vitex negundo, Medicago sativa (Alfalfa), Capsicum annuum, Camellia sinensis, Magnolia kobus, Origanum vulgare, Cinnamomum camphora, Moringa oleifera, Eucalyptus hybrida, Piper nigrum, and Coriandrum sativum*[17–36].

Eichhornia crassipes (Water hyacinth) is a freshwater aquatic plant belonging to the family Pontederiaceae and is abundant in Bangladesh and the South Asian region. Water hyacinth remains the most widely distributed and vicious aquatic weed[37]. Water hyacinth extracts have shown many medicinal functions, including antimicrobial and antifungal activities[38,39]. Bioactive compounds like flavonoids, alkaloids, phenols, terpenoids, tannins, ferulic acid, and β-stigmasterol are found in the leaf extract of *E. crassipes*[40–42]. These compounds play a key role as reducing and capping agents during the synthesis procedure of Ag NPs. But the green synthesis of Ag NPs using *Eichhornia crassipes* in Bangladesh remains largely unexplored, and their antimicrobial efficacy against clinically relevant bacterial and fungal pathogens has not been comprehensively evaluated.

The primary objective of this study was to synthesize biologically active silver nanoparticles (Ag NPs) using *Eichhornia crassipes* leaf extract (Fig. 1), an abundant, low-cost, and environmentally sustainable botanical resource[43]. To the best of our knowledge, this is the first report from Bangladesh on the synthesis of Ag NPs mediated by *E. crassipes* leaves. The nanoparticles were characterized using Ultraviolet–visible (UV–vis) spectroscopy and Fourier transform infrared (FTIR) spectroscopy to confirm their formation, physicochemical properties, and associated functional groups. In addition, the study evaluated the antibacterial and antifungal activities of the *E. crassipes*-derived Ag NPs, with a particular focus on Multidrug-Resistant (MDR) uropathogens associated with Urinary Tract Infections (UTIs). These studies have demonstrated that extracts from this plant are capable of producing Ag NPs with antimicrobial properties. Nevertheless, the available information on this process remains limited[44].

Materials and procedures

Materials

Mature, disease-free, the verdant foliage of *Eichhornia crassipes* was used as the plant material in this study. The reagents and substances employed in this investigation were all of analytical grade. Ethanol was bought from Merck, Germany. Sodium chloride (NaCl) and silver nitrate ($AgNO_3$) 99.99% were procured from Sigma, Germany. $AgNO_3$ and 70% ethanol were employed for biochemical assays and sterilization. Culture media preparation included MacConkey agar cultures, providing a bacterial habitat rich in nutrients. Falcon tubes, Eppendorf tubes, an inoculating loop, and a pipette were used for sample handling and quantification. Every experimental operation was conducted in a Laminar Air Flow cabinet equipped with BSL-2 for aseptic conditions to prevent contamination. Before characterizing the silver nanoparticles, UV-Spectroscopy and FTIR were used.

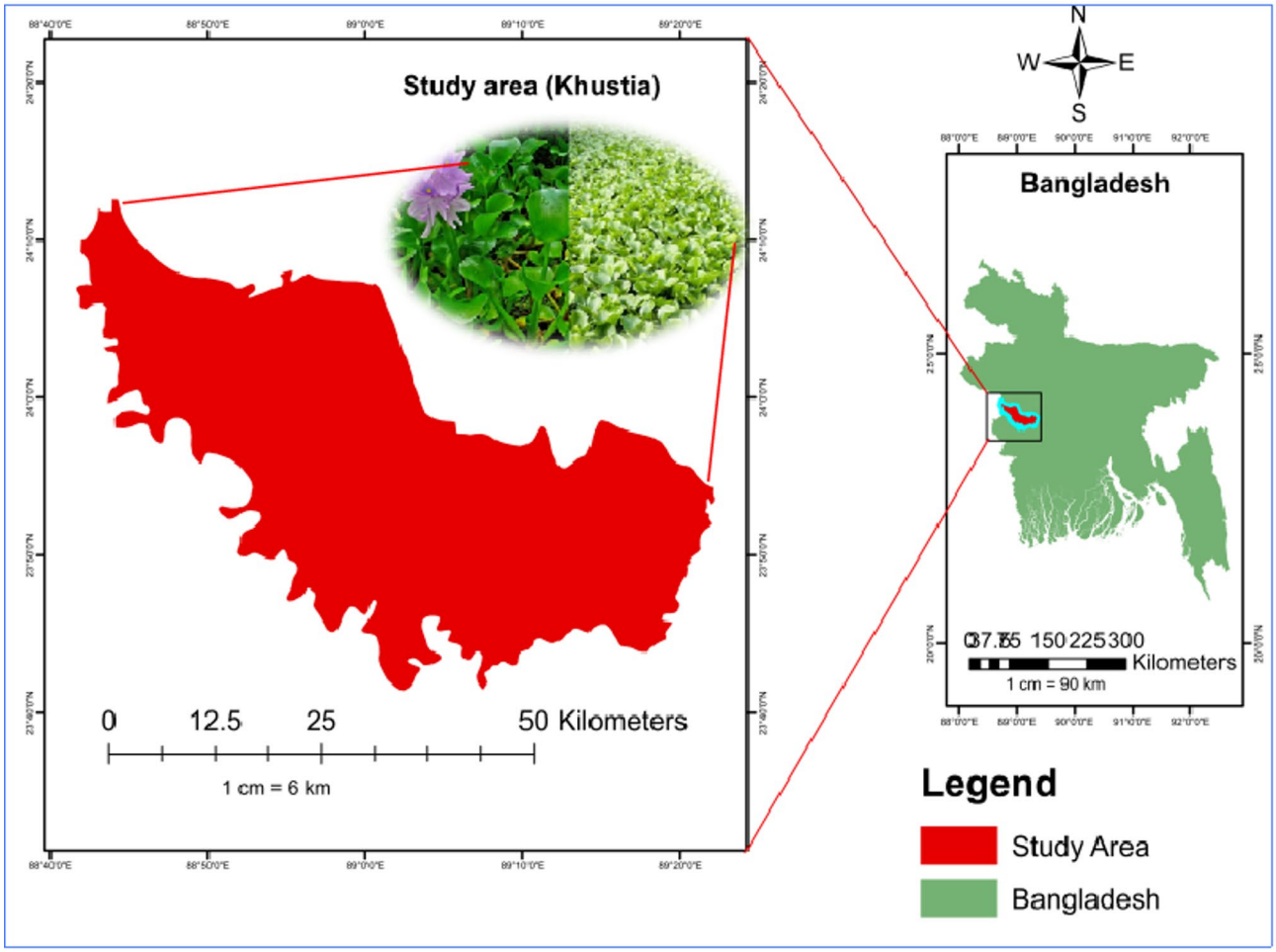

Fig. 1. Study area map showing the sample collection from the Islamic University, Kushtia, Bangladesh.

Before experimentation, surfaces and instruments were sterilized using UV light (Ultraviolet light). Bacterial growth and density were quantitatively assessed using measure the zone of inhibition, and statistical analysis.

All chemicals and culture media used in this study were of analytical grade. Sodium chloride (NaCl; ≥ 99% purity) and silver nitrate ($AgNO_3$; ≥ 99% purity) were procured from a certified commercial supplier. Double-distilled water and deionized water were used throughout the synthesis to ensure the absence of ionic contaminants. The *Eichhornia crassipes* leaf extract was prepared from freshly collected, thoroughly washed plant materials without any chemical additives.

Microbiological media and biochemical reagents, including MacConkey agar, blood agar, citrate, urea, lysine decarboxylase, coagulase reagent, novobiocin disks, motility medium, optochin disks, CAMP reagents, esculin medium, and Mueller–Hinton Agar, were of microbiological grade and supplied by standard manufacturers following CLSI-recommended quality specifications. Potato Dextrose Agar (PDA) used for antifungal assays was also of microbiological grade. All materials were used as supplied, without further purification.

Procedures

Processing of plant material and extract

The mature, healthy, and disease-free leaves of *Eichhornia crassipes* were collected in December 2023 from a freshwater body located on the campus of the Islamic University, Kushtia. The plant material was taxonomically identified and authenticated by the Department of Biotechnology and Genetic Engineering, and a voucher specimen was deposited under the accession number IU/BGE 022,024 for future reference. To ensure the removal of all surface contaminants, the collected leaves were initially rinsed with filtered water to eliminate adhered soil and particulate debris, followed by thorough washing with double-distilled water. After cleaning, the leaves were weighed at 4 g, air-dried at room temperature to remove excess moisture, and then cut into small pieces using sterilized scissors to increase the surface area for efficient phytochemical extraction.

The processed leaf material was transferred into a 500 mL borosilicate beaker containing 200 mL of double-distilled water. The mixture was gently stirred to ensure uniform dispersion and subsequently heated to a boil for 25 min using an electric heater. This thermal extraction facilitated the release of essential phytoconstituents, such as phenolics, flavonoids, and other reducing agents, responsible for nanoparticle synthesis. After heating, the mixture was allowed to cool naturally to room temperature, ensuring minimal thermal degradation of heat-

labile biomolecules. The extract was then filtered through Whatman No. 1 filter paper to remove fibrous residues and particulate material. The resulting clear filtrate was collected in a 250 mL Erlenmeyer flask and stored under refrigeration for subsequent synthesis and characterization steps.

Silver nitrate solution preparation

To prepare a 1200 mL 1 mM $AgNO_3$ solution, 0.204 g of $AgNO_3$ powder was added to 1.2 L of double-distilled water (Fig. 2). The solutions were adequately combined for reuse. Stored in a dark cabinet in tightly sealed, dark-colored (amber) glass bottles to prevent light-induced decomposition.

The $AgNO_3$ concentration (1 mM) was selected based on precedent in plant-mediated silver nanoparticle synthesis and because it supplies sufficient Ag^+ to promote rapid nucleation while limiting excessive growth and aggregation. To determine the optimal extract: $AgNO_3$ ratio, we screened ratios of 1:1, 1:2, and 1:4 (v/v) and monitored nanoparticle formation by UV–vis spectroscopy (SPR), and preliminary antimicrobial activity. The 1:2 (v/v) ratio yielded the most pronounced and narrow SPR peak (indicative of uniform formation), a smaller mean particle diameter, and superior antimicrobial efficacy; consequently, this ratio was used for all subsequent characterizations and biological tests.

Silver nanoparticles (Ag NPs) synthesis

For the reduction of Ag^+ ions, 5 mL of *Eichhornia crassipes* leaf extract was added to 95 mL of an aqueous solution containing 1 mM silver nitrate. The change of color from colorless to brown indicated that silver nitrate had been reduced to silver ions (Fig. 3). Spectrophotometric analysis also verified the production of silver nanoparticles. For 60 min, the completely diluted mixture was centrifuged at 10,000 rpm (Rotations Per Minute). Following the disposal of the liquid supernatant, the resulting particle was re-dispersed in deionized water. To eliminate any residual substances adsorbed onto the surface of the Ag NPs, the centrifugation process was repeated two to three times[45,46].

Assessment of the silver nanoparticle size

Different parameters affect the synthesis of silver nanoparticle size, including:

(a) The leaf extract (Ratio of silver nitrate):

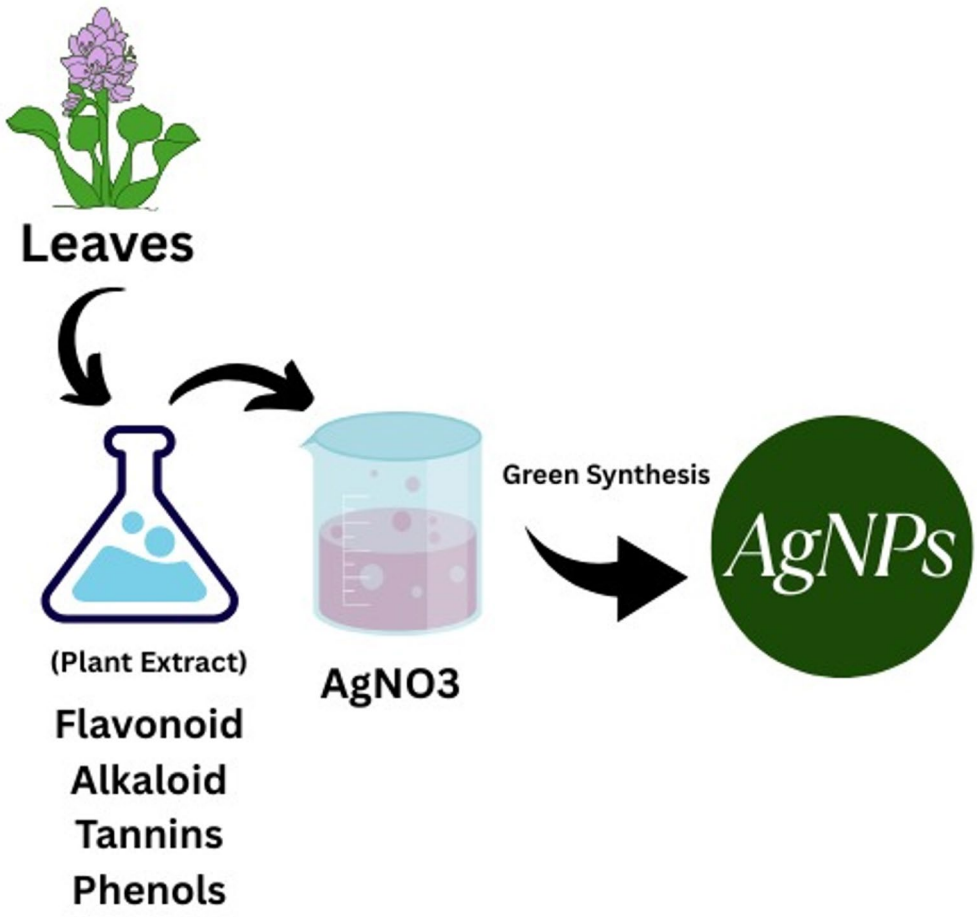

Fig. 2. Procedure for synthesizing silver nanoparticles from *Eichhornia crassipes* plant leaves.

Fig. 3. The color shift from colorless to brown indicated the synthesis of Ag NPs.

The different volumes of the ratio of silver nitrate affected the size of the synthesized Ag NPs with leaf extract and were investigated at several volumes (leaf extract: silver nitrate), which are (1:2, 1:4, 1:6, and 1:10).

(b) Time of Reaction:

The duration of the reaction influenced the generation of Ag NPs at different times studied (30 and 60 min).

Evaluation of silver nanoparticle properties

UV–vis spectra analysis

Periodically, samples were examined for Ultraviolet–Visible (UV–vis) spectroscopy examinations [UV-1800 spectrophotometer (Shimadzu, Japan)] at room temperature with a resolution of to observe the optical properties of biosynthesized silver nanoparticles range between 200 and 1200 nm. The UV–vis spectra of the reaction medium were measured after a tiny portion of the sample was diluted into deionized water in order to track the reduction of pure Ag + ions. In a test tube, 1 mL of the substance was pipetted, mixed with 4 mL of deionized water, and then allowed to sit at room temperature for examination[46].

Fourier transform infrared spectroscopy (FTIR)

A Perkin Elmer spectrum and an FTIR spectrometer (Shimadzu FTIR–8400–S) with the universal Attenuated Total Reflection (ATR) sampling accessory were used to measure the FTIR spectra to assess the functional groups present within green-synthesized Ag NPs. The transmission mode used for the measurements has a range of 4000–400 cm^{-1} and a resolution of 4 cm^{-1}, ensuring that each sample under analysis has a total of 50 scans[47].

Antibacterial study

Isolation and identification of UTI isolates

Between April and December 2024, a total of 50 urine samples that tested positive for culture revealed the presence of uropathogenic bacteria, including *Escherichia coli* (n = 14), *Klebsiella spp.* (n = 11), *Pseudomonas spp.* (n = 13), and *Staphylococcus spp.* (n = 12). All isolates were clinical strains collected from patients with suspected urinary tract infections at Kushtia Sadar Hospital in Bangladesh. Urine samples were taken midstream using sterile plastic containers. The samples were immediately processed for multiple analyses, including culture, Gram staining, and antibiotic susceptibility testing[48] (Table 1). The samples were inoculated on MacConkey

Samples	Tetracycline	Azithromycin	Cloxacillin	Levofloxacin	Doxycycline
N4 EF	R	S	S	S	S
N5 EF	R	S	S	S	S
N6 EF	R	S	S	S	S
N7	R	R	S	S	R
N8	R	R	S	S	R
N9	R	R	S	S	R

Table 1. Antibiotic sensitivity of six bacterial isolates. *Here, S represents Sensitivity and R represents resistance.

agar and Blood agar within one hour of being sampled. Under the microbe type, the incubation of the plates lasted 24–48 h at 37 °C under both aerobic and anaerobic conditions. Depending on whether the bacteria were Gram-positive or Gram-negative, typical microbiological examinations were performed on the different isolates. The Triple Sugar Iron (TSI) test, indole, citrate, urea, lysine decarboxylase, oxidase, and motility tests were used to detect Gram-negative bacteria. However, tests using catalase, coagulase, novobiocin, optochin disk, Cyclic Adenosine Monophosphate (CAMP), and esculin agar were performed for Gram-positive bacteria[49]. Clinical strains of these microorganisms lack unique ATCC or accession numbers since they were extracted from patient samples.

Antibacterial sensitivity assay

The disc diffusion assay was used to measure the antimicrobial action against MDR bacteria. Using sterile cotton swabs, UTI pathogens were cultured overnight on the surface of sterile Mueller–Hinton agar plates. The solid agar medium was covered with discs impregnated with varying quantities of silver nanoparticles (15, 30, 45, and 60 µg disc-1). Gently press and incubate for 24 h at 37 ± 2 °C[50].

Determination of MIC and MBC values

The antibacterial potential of the synthesized silver nanoparticles was further assessed through Minimum Inhibitory Concentration (MIC) and Minimum Bactericidal Concentration (MBC) assays. MIC determination was performed using the standard broth microdilution method. Briefly, bacterial isolates were grown overnight and adjusted to a 0.5 McFarland standard (≈1×10^8 CFU/mL). Serial two-fold dilutions of the silver nanoparticles were prepared in sterile nutrient broth, followed by inoculation with the bacterial suspension. The tubes were incubated at 37 °C for 24 h.

(a) MIC determination:

After incubation, the tubes were examined for turbidity. The MIC was defined as the lowest concentration showing no visible turbidity, signifying complete inhibition of bacterial growth. When visual interpretation was uncertain, absorbance was measured spectrophotometrically at 600 nm, and the concentration showing no increase in optical density compared to the negative control was recorded as the MIC value.

(b) MBC determination:

To determine the MBC, samples from tubes showing no visible growth were streaked onto fresh Mueller–Hinton agar plates and incubated at 37 °C for 24 h. The MBC was recorded as the lowest concentration that produced no bacterial colonies, indicating bactericidal activity. This combined turbidity assessment, spectrophotometric measurement, and plate count confirmation ensured reliable determination of MIC and MBC values for all UTI isolates tested.

Antifungal study

Fungal strain isolation and identification

Fungus-infected portions of vegetables were collected and cultured on Potato Dextrose Agar (PDA) medium, followed by incubation at 25 °C for approximately three days. Microscopic examination and morphological characterization of the cultured phytopathogenic fungus after incubation identified it as *Fusarium oxysporum.*

Dose concentration and test plate preparation

The poisoned plate (poisoned food) technique was employed to evaluate the antifungal activity of the extracted essential oil against the isolated *Fusarium oxysporum*. Ag NPs synthesized from *Eichhornia crassipes* leaf extract, at concentrations ranging from 1 to 32 µg/mL, were incorporated to prepare the treatment dosages. Sterilized Potato Dextrose Agar (PDA) medium was poured into sterile Petri dishes to prepare the test plates. After solidification, a 0.5 cm diameter mycelial disc was aseptically transferred, inverted, to the center of each plate. A control plate without any treatment was also maintained. The growth of the fungal colonies was observed at 24 h intervals during incubation at 25 °C until the control plate was completely covered with fungal growth. All treatments were performed in triplicate.

Statistical analysis

All quantitative results, encompassing zones of inhibition, minimum inhibitory concentration (MIC), Minimum Bactericidal/Fungicidal Concentration (MBC/MFC), and antifungal growth inhibition percentages, are reported as mean ± standard deviation (SD) derived from three separate samples (n = 3). Variations among treatment groups (e.g., varying concentrations of silver nanoparticles for each bacterial or fungal strain) were assessed

using one-way analysis of variance (ANOVA) accompanied by Tukey's post hoc test. Statistical significance was defined as $p < 0.05$. Statistical analyses were conducted utilizing SPSS version 20.0; IBM Corp., USA.

Specimen collection, identification, ethical approval, and legal compliance

Eichhornia crassipes (Mart.) Solms, an enormous and non-endangered aquatic species, was collected from publicly available water bodies in the Islamic University, Kushtia-7003, Bangladesh; Global Positioning System (GPS) coordinates: approximately 23.722734, 89.148202″ E in November 2023. Since the species is invasive and not under protection in Bangladesh, specific collection permits were not required. The plant was identified and authenticated by Farjana Sultana Primu, Department of Biotechnology and Genetic Engineering, Faculty of Life Science, Gopalganj Science and Technology University, Gopalganj-8100, Bangladesh, and a voucher specimen (Specimen No. EC-01.11.2023) has been deposited in the herbarium of the Department of Biotechnology and Genetic Engineering, Medical and Environmental Biotechnology Lab, Islamic University, Kushtia-7003, Bangladesh, in November 2023. The species is an invasive and non-endangered aquatic plant, not listed under the International Union for Conservation of Nature (IUCN) Red List of Threatened Species or the Convention on International Trade in Endangered Species of Wild Fauna and Flora (CITES). Therefore, no special permission was required for its collection. All sampling activities were conducted responsibly in accordance with the IUCN Policy Statement on Research Involving Species at Risk of Extinction and the national environmental regulations of Bangladesh. Furthermore, all procedures involving human-derived samples were carried out in accordance with institutional and national ethical standards and the Declaration of Helsinki. The collection and use of clinical samples were approved by the Ethical Review Committee of Kushtia Sadar Hospital, Kushtia, Bangladesh. Written informed consent was obtained from all patients and their legal guardians before sample collection. All data and samples were anonymized before use.

Result

Analysis of UV vis spectroscopy

Ag NPs formation was observed by a color change in the solution (from colorless to yellow to brown) when combining leaf extract and silver nitrate ($AgNO_3$) in different ratios (1:2, 1:4, 1:6, and 1:10). The Surface Plasmon Resonance (SPR) peaks observed in Fig. 4 at 468 nm with an absorbance of 1.516 for the 1:2 ratio (60 min), 454 nm with an absorbance of 1.029 for 1:4, 467 nm with an absorbance of 1.132 for 1:6, and 465 nm with an absorbance of 0.893 for 1:10 indicated silver nanoparticle formation, actual absornance values are stated in supplementary file (Table S1). In Fig. 5, with peaks at 454 nm (0.546 absorbance) for 1:2, 476 nm (0.722) for 1:4, 483 nm (0.868) for 1:6, and 480 nm (0.856) for 1:10 at 30 min, the spectra were not fully specific, actual absornance values are stated in supplementary file (Table S2). The Surface Plasmon Resonance (SPR) data and absorbance results indicated that the 1:2 ratio with 60 min stirring produced the highest concentration and size of Ag NPs.

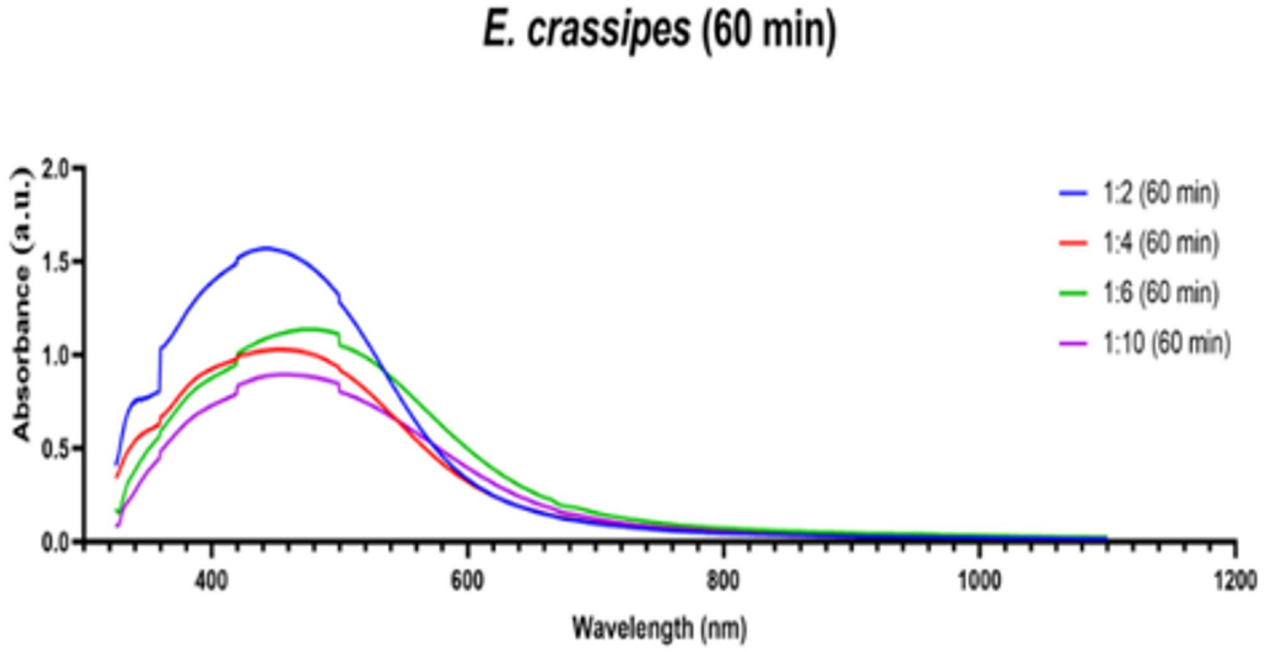

Fig. 4. UV–vis spectra of the synthesized silver nanoparticle sample at 1:2, 1:4, 1:6, and 1:10 ratios at 60 min. Here, 1:2 ratios produce the highest concentration and size of Ag NPs.

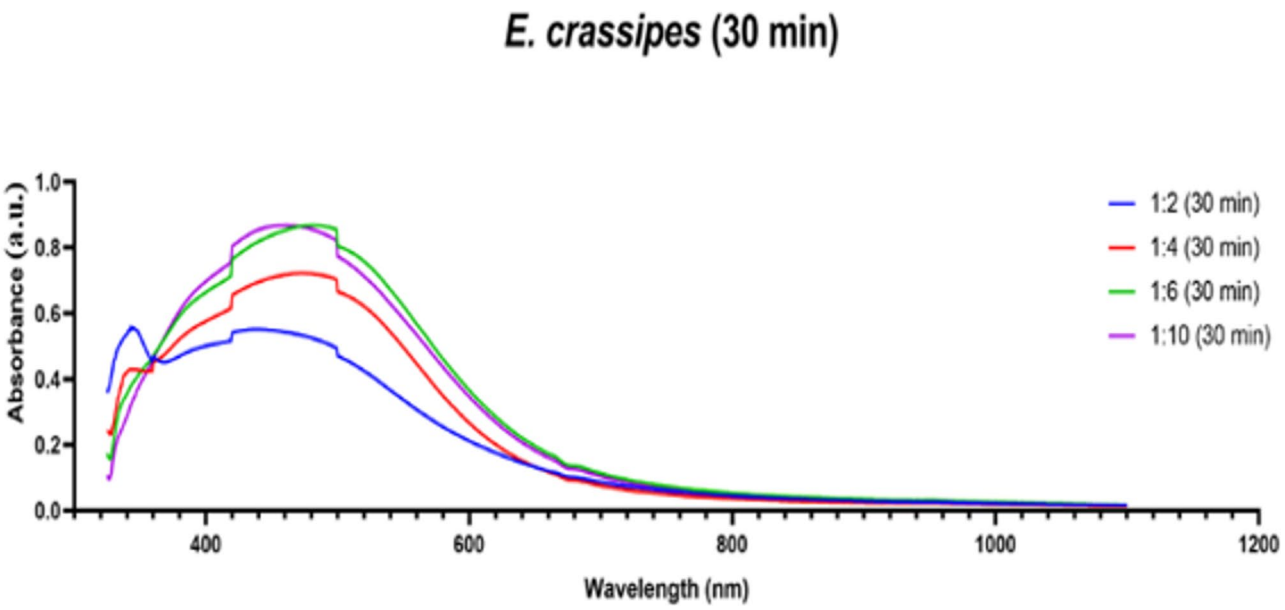

Fig. 5. UV–vis spectra of synthesized silver nanoparticle sample at 1:2, 1:4, 1:6 and 1:10 ratio at 30 min.

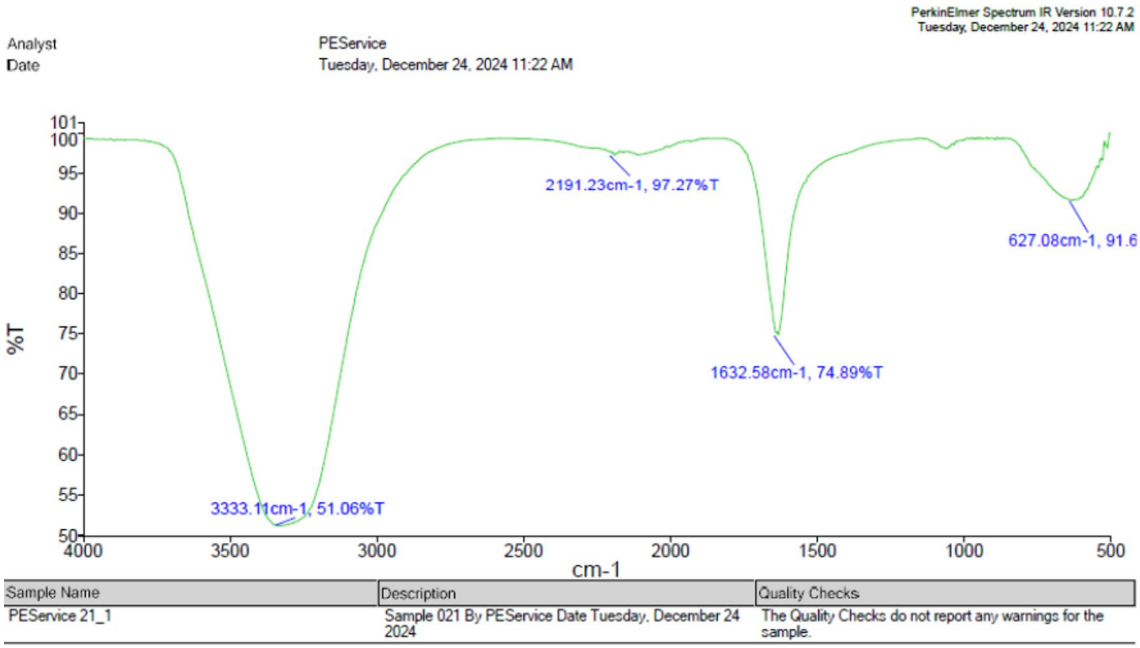

Fig. 6. FTIR spectrum of *Eichhornia crassipes* extracts and Ag NPs.

Fourier transform infrared (FTIR) analysis

Figure 6 illustrates the FTIR spectra of the boiled *Eichhornia crassipes* plant extract and Ag NPs. The spectrum exhibits several prominent absorption peaks corresponding to specific functional groups present in the sample. 3333.11 cm^{-1} (51.06%T): This broad peak is indicative of the presence of an O–H stretch, likely from an alcohol or carboxylic acid group. 2191.23 cm^{-1} (97.27%T): This sharp peak is characteristic of a C≡C stretch, suggesting the presence of an alkyne functional group. 1632.58 cm^{-1} (74.89%T): This peak is likely due to a C = O stretch, indicating the presence of a carbonyl group (e.g., in a ketone, aldehyde, or ester). 627.08 cm^{-1} (91.6%T): This peak is indicative of a C–Cl stretch, suggesting the presence of a chlorinated compound. The spectrum also shows several other peaks of varying intensities, which could be attributed to different functional groups or molecular vibrations. For improved clarity and cross-reference, the major FTIR absorption peaks of the dried *Eichhornia crassipes* leaf extract and the synthesized Ag NPs are summarized numerically in Table 4, actual absornance values are stated in supplementary file (Table S3). The spectrum includes a note indicating that the

quality checks did not report any warnings for the sample. This suggests that the spectrum is of good quality and can be reliably used for further analysis.

Bactericidal activity of Ag NPs

Table 1 shows the antibiotic sensitivity results of six bacterial samples isolated from medical waste against tetracycline, azithromycin, cloxacillin, levofloxacin, and doxycycline. The bactericidal efficacy of green-synthesized Ag NPs was evaluated by measuring the zone of inhibition (in mL) around bacterial cultures after an incubation phase. The results are presented in Table 2, comparing the effects of Ag NPs at different concentrations on MDR bacterial strains MEBTN 4(EF), MEBTN 5(EF), and MEBTN 6(EF) alongside the positive and negative controls. No bactericidal effects were observed in either the positive or negative control.

In Table 2, no bactericidal activity was observed in the positive control (P) and negative control (N), as the zone of inhibition for both was 0 mm. The zone of inhibition increased with increasing Ag NPs concentration, indicating a dose-dependent bactericidal effect, which means that the growth of individual MDR bacteria can be inhibited by Ag NPs, depending on the quantity used. The higher the dose of concentration, the bigger the zone of blockage. At 60 µg/ml, the maximum inhibition was observed: 10 ± 0.1 mm for MEBTN 4(EF), 11 ± 0.118 mm for MEBTN 5(EF), and 13 ± 0.1 mm for MEBTN 6(EF) (Figs. 7 and 8).

MEBTN 6(EF) was the most sensitive strain, with the largest zone of inhibition (13 ± 0.1 mm) at a concentration of 60 µg/ml of Ag NPs. The sensitivity to Ag NPs was also notable in MEBTN 5(EF) and MEBTN 4(EF), with inhibition zones of 11 ± 0.118 mm and 10 ± 0.1 mm, respectively, at the highest Ag NPs concentration of 60 µg/ml (Figs. 7 and 8). The MIC for all bacterial strains MEBTN 4(EF), MEBTN 5(EF), and MEBTN 6(EF) was determined to be 15 µg/ml, with corresponding zones of inhibition of 3 ± 0.153 mm MEBTN 4(EF), 7 ± 0.1 mm MEBTN 5(EF), and 6 ± 0.1 mm MEBTN 6(EF).

The results indicate that green-synthesized Ag NPs demonstrate substantial bactericidal properties against MDR bacteria in a concentration-dependent manner. The most effective concentration for inhibiting bacterial growth was 60 µg/ml, particularly against the MEBTN 6(EF) strain, which displayed the largest zone of inhibition. These findings highlight the potential of Ag NPs as an effective antimicrobial agent against antibiotic-resistant bacterial strains (Fig. 9).

Determination of antifungal activity

The fungal colony diameters were measured after 3 and 5 days of incubation, and the percent growth inhibition of the fungal mycelium was calculated using the following formula:

$$\text{Inhibition of mycelial growth, I (\%)} = \text{C} - \text{T/C} \times 100$$

where the inhibition percent C is colony diameter in control (cm), and T is colony diameter in treatment (cm).

Determination of antifungal activity using the poisoned food method

The poisoned food method is a laboratory screening technique used to evaluate how strongly a substance (plant extract, essential oil, nanoparticle, or chemical) inhibits fungal growth when incorporated into a nutrient medium.

The antifungal activity of citronella oil was assessed by measuring the zone of inhibition in centimeters (Table 3) with a transparent scale, followed by adequate incubation. The MIC was assessed as 18 µg/mL, which represents the lowest concentration at which complete fungal growth inhibition was carried out. The fungal growth resumed below this concentration (Tables 4, 5). These experiments were conducted using the poisoned food technique. Therefore, silver nanoparticles synthesized from *Eichhornia crassipes* leaf extract, exhibiting an MIC of 18 µg/mL, can be considered effective fungicides. The antimicrobial profiles of the synthesized compounds against both bacterial and fungal pathogens are summarized in the comparative Table 6. Overall, the compounds exhibited a broad-spectrum activity, with particularly high potency observed against Gram-positive strains compared to fungal isolates.

Discussion

The present study investigated the potential of *Eichhornia crassipes* leaf extract to synthesize Ag NPs and their biomedical applications in controlling MDR bacterial pathogens through a green synthesis approach. Subsequently, the antibacterial efficacy of the synthesized nanoparticles was evaluated against antibiotic-resistant

Dose identification	Concentration	Zone of inhibition (mm; mean ± SD, n = 3)		
		MEBTN 4(EF)	MEBTN 5(EF)	MEBTN 6(EF)
P	Positive control	0.00 ± 0.00 mm	0.00 ± 0.00 mm	0.00 ± 0.00 mm
N	Negative control	0.00 ± 0.00 mm	0.00 ± 0.00 mm	0.00 ± 0.00 mm
I	15 µg/ml	3 ± 0.153 mm	7 ± 0.1 mm	6 ± 0.1 mm
II	30 µg/ml	5 ± 0.577 mm	7 ± 0.1 mm	8 ± 0.115 mm
III	45 µg/ml	9 ± 0.513 mm	10 ± 0.1 mm	10 ± 0.173 mm
IV	60 µg/ml	10 ± 0.1 mm	11 ± 0.118 mm	13 ± 0.1 mm

Table 2. Bacterial efficacy of green-synthesized silver nanoparticles (Ag NPs). *Here, values are expressed as mean ± SD (n = 3); "0" indicates no measurable inhibition in any replicate.

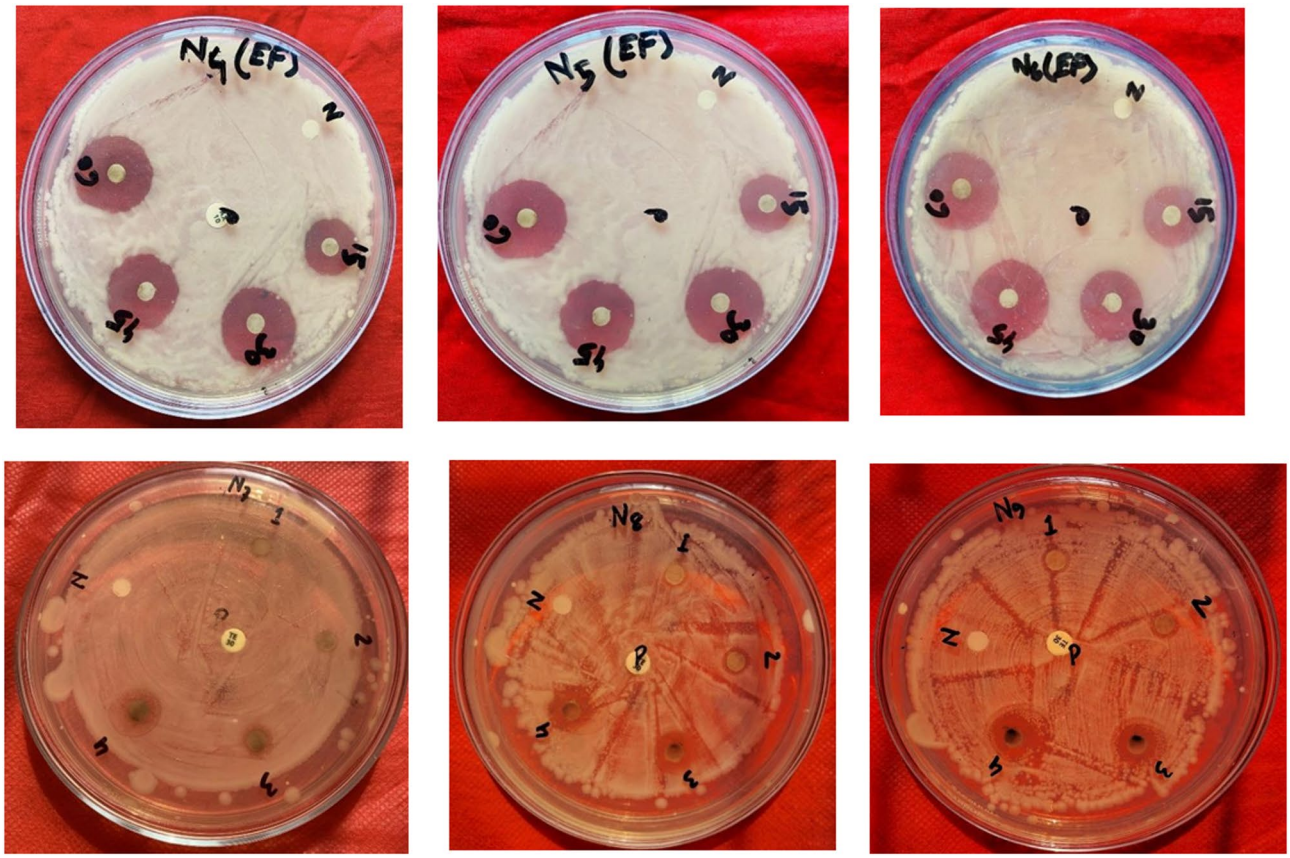

Fig. 7. Antibiotic susceptibility of isolated bacterial strains. Susceptibility of MEBTN 4(EF) to MEBTN9 bacteria to Tetracycline, Azithromycin, Cloxacillin, Levofloxacin, and Doxycycline antibiotics.

Fig. 8. Petridishes with bacterial zone of inhibition N4(EF), N5(EF), N6(EF) represent the MEBTN 4(EF), MEBTN 5(EF) and MEBTN 6(EF) respectively.

bacteria, particularly those associated with UTIs. Another objective of this work was to explore the possibility of employing *Eichhornia crassipes* leaf extracts as an environmentally benign substitute for nanoparticle manufacturing[51–53]. The administration of antimicrobial treatment in hospital settings is constantly challenged by MDR bacteria, which constitute a rising burden[54,55]. The antibacterial properties of silver nanoparticles (Ag NPs) make them useful for treating microbial illnesses[56].

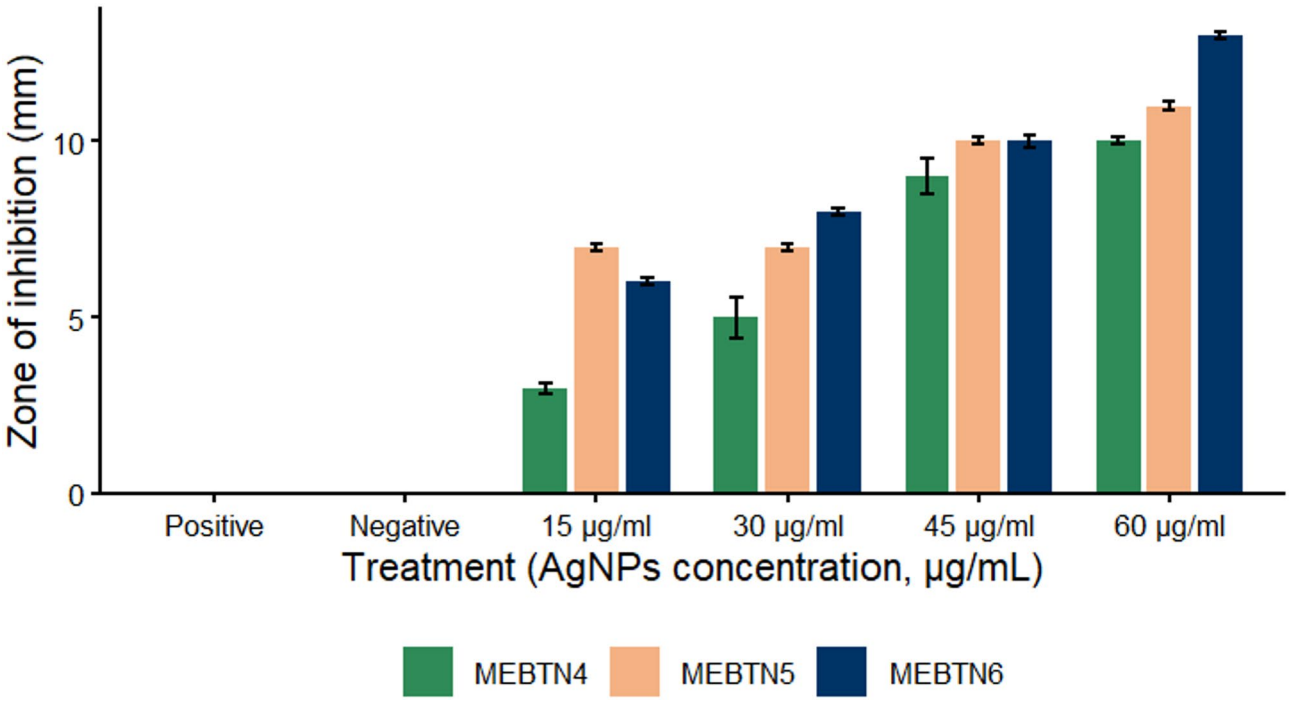

Fig. 9. The zone of inhibition for multidrug-resistant UTI isolates MEBTN4, MEBTN5, and MEBTN6 was assessed following treatment with *Eichhornia crassipes* leaf-extract-mediated silver nanoparticles (Ag NPs) at varying concentrations (15–60 µg/mL), alongside positive and negative controls. Data are presented as mean ± SD (n = 3).

Treatment		Colony diameter in cm ± SD
Oil extract	36 µg/ml	3.27 ± 0.19 cm
	18 µg/ml	2.19 ± 0.14 cm
	12 µg/ml	0 cm
	6 µg/ml	0 cm
	3 µg/ml	0 cm
	2 µg/ml	0 cm

Table 3. Diameter of inhibition zone (cm) of *Eichhornia crassipes* leaf (oil) extract-derived Ag NPs (µg/ml). *Here, values are mean ± SD (n = 3). 0 cm indicates complete inhibition of fungal growth (no visible colony) in all replicates.

Peak position (cm^{-1})	Transmittance (%T)	Functional group assignment	Interpretation/notes
3333.11 cm^{-1}	51.06%T	O–H Stretch	Broad peak indicating the presence of alcohol or carboxylic acid O–H groups
2191.23 cm^{-1}	97.27%T	C≡C Stretch (Alkyne)	Sharp peak characteristic of alkyne functional groups
1632.58 cm^{-1}	74.89%T	C = O Stretch	Suggests the presence of a carbonyl-containing compound (ketone, aldehyde, ester)
627.08 cm^{-1}	91.60%T	C–Cl Stretch	Indicates a chlorinated compound or halogen-containing functional group

Table 4. Summary of FTIR peaks.

Color change

The transformation of reaction mixture of $AgNO_3$ and leaf extract color was demonstrated to be the first evidence of nanoparticle production[57]. *Eichhornia crassipes* plants have been shown to contain significant concentrations of Quercetin, a potent antioxidant flavonoid. These chemical releases hydrogen from the molecule through hydroxyl (-OH) groups that exhibit keto-enol tautomerism. It is thought that silver ions are reduced to a metallic form by the free hydrogen[58]. Gradual changes in color from colorless silver nitrate solution to yellow to deep brown were seen because of the excitation of surface plasmon vibrations (Fig. 3)[59]. This hypothesis is supported

Plant source	Target bacteria	AgNP size (nm)	Assay method	Antibacterial efficacy	References
Eichhornia crassipes	*E. coli*	Unidentified	Agar well diffusion	IZ: 6.2–13.1 mm; MIC: 15 µg/mL	*This study
Azadirachta indica	*E. coli*	33	Agar well diffusion	IZ: 17.7–18.7 mm MIC: 390–780 µg/mL	Chinnasamy et al. (2021)
Zingiber officinale	*E. coli*	200.5	Agar well diffusion	IZ: 20.83 ± 0.53 µg/mL	Ramzan et al. (2024)
Ocimum sanctum	*E. coli*	55	Agar well diffusion	IZ: 15 mm MIC: 32–64 µg/mL	Gautam et al. (2023)
Curcuma longa	*E. coli*	5–25	Agar well diffusion	IZ:14–22.76 mm MIC: 100 µg/mL	Jayarambabu et al. (2019)

Table 5. Comparative antibacterial activity (mm for Zone of inhibition and µg/mL for Minimal inhibitory concentration) of plant-mediated silver nanoparticles (nm). *IZ: Zone of inhibition; MIC: Minimal inhibitory concentration.

Antimicrobial agent	Target microorganism (s)	Method	MIC (µg/mL)	Maximum inhibition observed	Key observation
Silver nanoparticles (SNPs)	MEBTN 4(EF)	Agar diffusion	15	10 ± 0.1 mm (60 µg/mL)	Dose-dependent bactericidal activity
Silver nanoparticles (SNPs)	MEBTN 5(EF)	Agar diffusion	15	11 ± 0.118 mm (60 µg/mL)	Moderate sensitivity
Silver nanoparticles (SNPs)	MEBTN 6(EF)	Agar diffusion	15	13 ± 0.1 mm (60 µg/mL)	Most sensitive bacterial strain
Positive control	Bacteria	Agar diffusion	–	0 mm	No inhibition
Negative control	Bacteria	Agar diffusion	–	0 mm	No inhibition
Citronella oil	Fungal isolate	Poisoned food technique	18	Complete growth inhibition	Effective antifungal agent
SNPs (*E. crassipes*)	Fungal isolate	Poisoned food technique	18	Complete growth inhibition	Effective green fungicide

Table 6. Combine bacterial and antifungal results in a summarized comparative form; improve readability.

by a recent study by Peidaei and Farideh et al. (2025), which reported the transformation from green to dark brown provide a clear indication of the formation of Ag NPs using *Eichhornia crassipes* extract.

It is important to notice that the coloring intensifies and darkens with increasing temperature and that this rise is related to the reaction time. The huge changes from translucent to yellow and then to deep brown as the concentration rises, as has been demonstrated by[60,61]. No color change was recorded, suggesting that no nanoparticles were synthesized using the incubation procedure at 37 °C in the dark. This study supports the idea by Birla et al. (2013) that visible light is crucial for reducing silver ions, while its exact mechanism is yet unknown[62,63].

UV–vis spectroscopy

The primary step in characterizing Ag NPs was to scan a UV–visible spectrum[64]. 1.2 solutions agitated for 60 min produced better silver nanoparticles and displayed the highest intensity and wavelength movement of SPR peaks. Similarly, Venkatadri et al. (2020) reported the UV–visible spectra of *Zingiber officinale* and *Curcuma longa* extracts, exhibiting absorption between 350 and 430 nm.

In our investigation, the spectrum analysis peak at 468 nm proves that the silver synthesized product is only Ag NPs. It was found that there was a plasmon shift and that absorbance increased with time (30 and 60 min), reaching a maximum absorbance at 60 min of reaction. Higher metallic silver concentrations have been linked to increases in absorbance, although larger particles are primarily responsible for the highest peak shift toward longer wavelengths[45]. However, the maximum absorbance value stopped increasing when reaction durations exceeded 60 min. The measurement of the highest peak amplitude revealed that the distribution of nanoparticle sizes is polydisperse[65,66]. The reason behind this variation in the size of the synthesized nanoparticles is their aggregation state and impurities[63].

FTIR

When demonstrating the existence of biomolecule functional groups in an extract that act as capping and reducing agents, FTIR spectroscopy is frequently employed[64]. Accordingly, all samples showed the same number of distinctive peaks and intensity in the FTIR spectra of the dried extract and the synthesized silver (Ag). In the *Eichhornia crassipes* leaf extract, the stretching vibration of hydroxyl (–OH) groups in terpenoids, polyphenolic compounds with carboxylic chemicals, and alcohol functional groups is responsible for the wide band at 3333.11 cm^{-1} (51.06% T). The peak at 2191 cm^{-1} (97.27% T) could be attributed to the (CH) stretching band of the alkyne functional group[67], and the high-intensity peak at 1632.58 cm – 1 (74.89% T) is related to C = C and C = O vibrations of benzene rings and carbonyl groups of amino acids[68]. The peak at 627 cm^{-1} (91.6% T) is related to the C–Cl stretching vibrations of the chlorinated compound[69].

As a result, the corresponding polyphenolic groups have been identified as the primary reducing agents in the synthesis of Ag NPs[70]. The complete disappearance of this band following the bio-reduction might be due to the primary role of polyols and phenols in reducing Ag ions, which results in their oxidation to unsaturated carbonyl groups, leading to the broad peak 1632.58 cm^{-1} (74.89% T)[71]. The reaction between $AgNO_3$ and alcoholic groups (-OH) present in the *Eichhornia crassipes* leaf extract can be represented by[72].

$$2Ag + NO_3^- + ROH \rightarrow 2Ag0 + RO + 2HNO_3$$

According to FTIR studies, the carbonyl group of proteins and amino acids exhibits a greater affinity for Ag NPs, allowing them to form a coating on their surface. As a result, the surface-capped biomolecules stabilize the silver nanoparticles by preventing agglomeration. This implies that biological molecules may serve as agents that reduce and stabilize silver nanoparticles[73,74].

Antimicrobial activity against UTI pathogens

It is widely recognized that Ag ions and compounds are inorganic nanoparticles of interest and have powerful antimicrobial effects. Because of their resistance, new alternatives are needed to suppress some microbes[75]. The antibacterial efficacy of synthesized Ag NPs was evaluated against MEBTN4 (EF), MEBTN5 (EF), and MEBTN6 (EF), followed by the addition of different concentrations of Ag NPs, 15, 30, 45, and 60 µg/ml, respectively. Since these strains exhibit multidrug resistance, they are mostly associated with hospital-acquired infections. Strain MEBTN 6(EF) exhibited a significant zone of inhibition (13 ± 0.1 mm) at a concentration of 60 µg/ml of Ag NPs, supported by Kasithevar et al. (2017) (Table 2).

An increase in incubation time and temperature resulted in an enhanced zone of inhibition with rising concentrations of Ag NPs, indicating a dose-dependent bactericidal effect that varied with the bacterial strain. In general, the diameter of the inhibitory halo expanded with increasing Ag NPs concentration until reaching a maximum level. Notably, the greatest inhibition was observed at a concentration of 60 µg/mL of Ag NPs[45]. Along with environmental variables, size, shape, aggregation, and condition of Ag NPs all affect pH and the zone of inhibition. The suitability of nanoparticles for a specific antibacterial application is determined by the required rate of Ag^+ ion release. For a given mass of silver nanoparticles, smaller particle diameters provide a larger total surface area, thereby facilitating a more rapid ion release. When the cluster is coupled with a particular substrate or the particles are unstable in solution, the available surface area and the rate of ion release are reduced[76]. Ag NPs exhibit antibacterial activity primarily through the generation of Reactive Oxygen Species (ROS), including superoxide anions, hydroxyl radicals, and hydrogen peroxide[77]. These ROS disrupt cell membrane integrity, oxidize intracellular proteins, and induce DNA damage, collectively contributing to bacterial cell death[78]. In our study, antibacterial efficacy was assessed using the zone of inhibition method, where larger inhibition zones indicate greater susceptibility[79]. The stronger activity observed against MEBTN 6(EF) at 60 µg/ml may be attributed to its thinner peptidoglycan layer and higher membrane permeability, which facilitate greater penetration of Ag NPs and higher ROS-induced oxidative stress[78]. In contrast, the relatively lower inhibition in MEBTN 4(EF) at 15 µg/ml may result from a thicker cell wall or more effective antioxidant defense mechanisms[80]. The experiment unequivocally showed that gram-negative bacteria were more sensitive to Ag NPs than gram-positive bacteria. The difference in their cell wall construction may be due to this discrepancy[70]. The surface of the Ag NPs generates ROS or free radicals that compromise the integrity of the cell membrane by increasing its permeability, ultimately leading to cell death. Due to the strong peptidoglycan layer in their cell membrane, gram-positive bacteria are less sensitive to Ag NPs. On the other hand, Ag NPs infiltrate gram-negative bacteria due to the thin lipid layer in their cell membrane. The antibacterial activity of Ag NPs has been elucidated through various mechanisms. The mechanism of action is not fully understood; it is thought that these nanoparticles obstruct respiratory metabolic processes. They inhibit enzyme function by interacting with sulfur-containing proteins found in the bacterial cell membrane. Otherwise, they are known to interact with DNA's phosphorus moieties, which inactivate DNA replication[81–83]. Findings suggest that the Ag ion's positive charge interacts with the cell membrane's negative charge. Thus, Ag NPs accumulate in the membrane and lead to cell death[84]. Following treatment of the bacterial inocula with Ag NPs, the initially turbid yellow culture became translucent, clearly indicating growth inhibition. The Ag NPs treatment exhibited inhibitory effects on both Gram-positive and Gram-negative bacteria. The dose-dependent decline in microbial growth further demonstrates the susceptibility of these pathogens to Ag NP exposure. By calculating their MIC values against the corresponding bacterial inocula, the antibacterial activity was quantified. The MIC value is defined as the minimal concentration of nanoparticles at which no bacterial growth is detected. The antibacterial and antifungal activities of the synthesized AgNPs are summarized in a single comparative table (Table 5).

Our findings are consistent with earlier investigations that have demonstrated the antimicrobial potential of silver nanoparticles synthesized using plant extracts like *Peganum harmala* L, *Lysiloma acapulcensis*, *Aspergillus flavus*, and *Ziziphus ziziphus*[64,85–87]. Although morphological and size characterization by SEM or TEM was not performed in the present study, the novelty of Eichhornia crassipes–mediated silver nanoparticles lies in their green synthesis efficiency, phytochemical-mediated stabilization, and antimicrobial performance. Unlike many previously reported plant-based Ag NPs that require prolonged reaction times or elevated temperatures, the present synthesis achieved rapid nanoparticle formation under ambient conditions. However, the nanoparticles in our study exhibited very effective antibacterial activity at a low concentration (60 µl/ml), likely due to the unique chemical composition of *Eichhornia crassipes* leaves, which may enhance the antimicrobial properties of the Ag NPs.

Conclusion

Silver nanoparticles (Ag NPs) were successfully synthesized via a green route using *Eichhornia crassipes* leaf extract. Formation was confirmed by UV–vis spectroscopy and FTIR analysis, with the 1:2 extract to $AgNO_3$ ratio identified as the optimal synthesis condition. The Ag NPs exhibited pronounced antibacterial activity against *Escherichia coli* UTI isolates and significant antifungal activity against *Fusarium oxysporum*, with a clear dose–response relationship between nanoparticle concentration and microbial inhibition. These results demonstrate that *E. crassipes,* an abundant aquatic weed, represents a viable, low-cost, and environmentally friendly source

for large-scale production of biologically active Ag NPs. This green-synthesis approach offers a promising strategy for developing antimicrobial agents for biomedical and agricultural applications. Direct morphological and size analysis using SEM or TEM and identification of individual phytocompounds by GC–MS were not performed due to instrumental limitations. But FTIR analysis and supporting literature were used to propose the nanoparticle formation mechanism. Furthermore, we did not examine other biologically pertinent activities, such as antioxidant and anti-inflammatory effects, which would yield a more comprehensive understanding of the potential therapeutic profile of these nanoparticles. And we also did not conduct microscopic investigations (e.g., light or electron microscopy) to observe nanoparticle-induced morphological alterations in bacterial or fungal cells, which could further corroborate the suggested antibacterial mechanism. The study ultimately did not investigate the potential cytotoxic effects of these nanoparticles on mammalian cells or their in vivo safety. On the other hand, the novelty of the work has been emphasized based on a synthesis approach, spectral characteristics, reaction efficiency, and antimicrobial efficacy. Future work should focus on detailed SEM or TEM, XRD, DLS, Zeta potential, GC–MS analysis, in vivo toxicity studies, mechanism elucidation, anti-cancer activity, ROS-related effects, and scale-up optimization, etc.

Data availability

The experimental data and results that support the findings of this study are available in supplementary word file (Table S1, S2, and S3).

Received: 10 October 2025; Accepted: 18 February 2026
Published online: 02 March 2026

References

1. Kumar, R., Ghoshal, G., Jain, A. & Goyal, M. Rapid green synthesis of silver nanoparticles (AgNPs) USING (*Prunus persica*) plants extract: Exploring its antimicrobial and catalytic activities. *J. Nanomed. Nanotechnol.* **08**(04), 1–8. https://doi.org/10.4172/2157-7439.1000452 (2017).
2. Ahmed, S., Ahmad, M., Swami, B. L. & Ikram, S. A review on plants extract mediated synthesis of silver nanoparticles for antimicrobial applications: A green expertise. *J. Adv. Res.* https://doi.org/10.1016/j.jare.2015.02.007 (2016).
3. Jalab, J., Abdelwahed, W., Kitaz, A. & Al-Kayali, R. Green synthesis of silver nanoparticles using aqueous extract of Acacia cyanophylla and its antibacterial activity. *Heliyon* https://doi.org/10.1016/j.heliyon.2021.e08033 (2021).
4. Ren, Y., Yang, H., Wang, T. & Wang, C. Bio-synthesis of silver nanoparticles with antibacterial activity. *Mater. Chem. Phys.* https://doi.org/10.1016/j.matchemphys.2019.121746 (2019).
5. Panda, S. K., Sen, S., Roy, S. & Moyez, A. Synthesis of colloidal silver nanoparticles by reducing aqueous $AgNO_3$ using green reducing agents. *Mater. Today Proc.* https://doi.org/10.1016/j.matpr.2017.10.206 (2018).
6. Rab Nawaz, H. Z. et al. Synthesis of silver/silver oxide heterostructures via partial reduction of $AgNO_3$ using a novel green reducing agent. *Ceram. Int.* **48**(24), 37194–37202. https://doi.org/10.1016/j.ceramint.2022.08.296 (2022).
7. Alowaiesh, B. F., Alhaithloul, H. A. S., Saad, A. M. & Hassanin, A. A. Green biogenic of silver nanoparticles using polyphenolic extract of olive leaf wastes with focus on their anticancer and antimicrobial activities. *Plants* **12**(6), 1410. https://doi.org/10.3390/plants12061410 (2023).
8. Swilam, N. & Nematallah, K. A. Polyphenols profile of pomegranate leaves and their role in green synthesis of silver nanoparticles. *Sci. Rep.* https://doi.org/10.1038/s41598-020-71847-5 (2020).
9. Bindhu, M. R., Umadevi, M., Esmail, G. A., Al-Dhabi, N. A. & Arasu, M. V. Green synthesis and characterization of silver nanoparticles from *Moringa oleifera* flower and assessment of antimicrobial and sensing properties. *J. Photochem. Photobiol. B Biol.* https://doi.org/10.1016/j.jphotobiol.2020.111836 (2020).
10. Renuka, R. et al. Biosynthesis of silver nanoparticles using *Phyllanthus emblica* fruit extract for antimicrobial application. *Biocatal. Agric. Biotechnol.* https://doi.org/10.1016/j.bcab.2020.101567 (2020).
11. Rohaizad, A. et al. Green synthesis of silver nanoparticles from *Catharanthus roseus* dried bark extract deposited on graphene oxide for effective adsorption of methylene blue dye. *J. Environ. Chem. Eng.* https://doi.org/10.1016/j.jece.2020.103955 (2020).
12. Andreia, C. & Ivanescu, B. Biosynthesis, characterisation and therapeutic applications of plant-mediated silver nanoparticles. *J. Serb. Chem. Soc.* https://doi.org/10.2298/JSC170731021C (2018).
13. Arshad, F. et al. Bioinspired and green synthesis of silver nanoparticles for medical applications: A green perspective. *Appl. Biochem. Biotechnol.* https://doi.org/10.1007/s12010-023-04719-z (2024).
14. Hussain, I., Singh, N. B., Singh, A., Singh, H. & Singh, S. C. Green synthesis of nanoparticles and its potential application. *Biotechnol. Lett.* **38**(4), 545–560. https://doi.org/10.1007/s10529-015-2026-7 (2016).
15. Rajan, R., Chandran, K., Harper, S. L., Yun, S. I. & Kalaichelvan, P. T. Plant extract synthesized silver nanoparticles: An ongoing source of novel biocompatible materials. *Ind. Crops Prod.* https://doi.org/10.1016/j.indcrop.2015.03.015 (2015).
16. Shahraki, S. H., Ahmadi, T., Jamali, B. & Rahimi, M. The biochemical and growth-associated traits of basil (*Ocimum basilicum* L.) affected by silver nanoparticles and silver. *BMC Plant Biol.* **24**(1), 92. https://doi.org/10.1186/s12870-024-04770-w (2024).
17. Vijayakumar, M., Priya, K., Nancy, F. T., Noorlidah, A. & Ahmed, A. B. A. Biosynthesis, characterisation and anti-bacterial effect of plant-mediated silver nanoparticles using *Artemisia nilagirica*. *Ind. Crops Prod.* https://doi.org/10.1016/j.indcrop.2012.04.017 (2013).
18. Ahmad, N. et al. Rapid synthesis of silver nanoparticles using dried medicinal plant of basil. *Colloids Surf. B Biointerfaces* https://doi.org/10.1016/j.colsurfb.2010.06.029 (2010).
19. Kannan, N., Mukunthan, K. S. & Balaji, S. A comparative study of morphology, reactivity and stability of synthesized silver nanoparticles using *Bacillus subtilis* and *Catharanthus roseus* (L.) G. Don. *Colloids Surf. B Biointerfaces* https://doi.org/10.1016/j.colsurfb.2011.04.024 (2011).
20. Supraja, S. et al. Green synthesis of silver nanoparticles from *Cynodon dactylon* leaf extract. *Int. J. ChemTech Res.* **5**(1), 271 (2013).
21. Banerjee, P., Satapathy, M., Mukhopahayay, A. & Das, P. Leaf extract mediated green synthesis of silver nanoparticles from widely available Indian plants: Synthesis, characterization, antimicrobial property and toxicity analysis. *Bioresour. Bioprocess.* https://doi.org/10.1186/s40643-014-0003-y (2014).
22. Jagajjanani Rao, K. & Paria, S. Green synthesis of silver nanoparticles from aqueous *Aegle marmelos* leaf extract. *Mater. Res. Bull.* https://doi.org/10.1016/j.materresbull.2012.11.035 (2013).
23. Bindhu, M. R. & Umadevi, M. Synthesis of monodispersed silver nanoparticles using *Hibiscus cannabinus* leaf extract and its antimicrobial activity. *Spectrochim. Acta A Mol. Biomol. Spectrosc.* https://doi.org/10.1016/j.saa.2012.09.031 (2013).
24. Zhang, Y., Cheng, X., Zhang, Y., Xue, X. & Fu, Y. Biosynthesis of silver nanoparticles at room temperature using aqueous aloe leaf extract and antibacterial properties. *Colloids Surf. A Physicochem. Eng. Asp.* **423**, 63. https://doi.org/10.1016/j.colsurfa.2013.01.059 (2013).

25. Leela, A. & Vivekanandan, M. Tapping the unexploited plant resources for the synthesis of silver nanoparticles. *Afr. J. Biotechnol.* **7**(17), 3162 (2008).
26. Prabhu, N., Raj, D. T., Yamuna Gowri, K., Ayisha Siddiqua, S. & Joseph Puspha Innocent, D. Synthesis of silver phyto nanoparticles and their antibacterial efficacy. *Dig. J. Nanomater. Biostruct.* **5**(1), 185 (2010).
27. Gardea-Torresdey, J. L. et al. Alfalfa sprouts: A natural source for the synthesis of silver nanoparticles. *Langmuir* https://doi.org/10.1021/la020835i (2003).
28. Li, S. et al. Green synthesis of silver nanoparticles using *Capsicum annuum* L. extract. *Green Chem.* https://doi.org/10.1039/b615357g (2007).
29. Loo, Y. Y., Chieng, B. W., Nishibuchi, M. & Radu, S. Synthesis of silver nanoparticles by using tea leaf extract from *Camellia sinensis*. *Int. J. Nanomed.* **7**, 4263. https://doi.org/10.2147/IJN.S33344 (2012).
30. Song, J. Y., Jang, H. K. & Kim, B. S. Biological synthesis of gold nanoparticles using *Magnolia kobus* and *Diopyros kaki* leaf extracts. *Process Biochem.* https://doi.org/10.1016/j.procbio.2009.06.005 (2009).
31. Sankar, R. et al. *Origanum vulgare* mediated biosynthesis of silver nanoparticles for its antibacterial and anticancer activity. *Colloids Surf. B Biointerfaces* https://doi.org/10.1016/j.colsurfb.2013.02.033 (2013).
32. Huang, J. et al. Biosynthesis of silver and gold nanoparticles by novel sundried *Cinnamomum camphora* leaf. *Nanotechnology* https://doi.org/10.1088/0957-4484/18/10/105104 (2007).
33. Prasad, T. N. V. K. V. & Elumalai, E. K. Biofabrication of Ag nanoparticles using *Moringa oleifera* leaf extract and their antimicrobial activity. *Asian Pac. J. Trop. Biomed.* https://doi.org/10.1016/S2221-1691(11)60096-8 (2011).
34. Dubey, M., Bhadauria, S. & Kushwah, B. S. Green synthesis of nanosilver particles from extract of *Eucalyptus hybrida* (Safeda) leaf. *Dig. J. Nanomater. Biostruct.* **4**(3), 537 (2009).
35. Paulkumar, K. et al. *Piper nigrum* leaf and stem assisted green synthesis of silver nanoparticles and evaluation of its antibacterial activity against agricultural plant pathogens. *Sci. World J.* **2014**, 829894. https://doi.org/10.1155/2014/829894 (2014).
36. Nazeruddin, G. M. et al. *Coriandrum sativum* seed extract assisted in situ green synthesis of silver nanoparticle and its antimicrobial activity. *Ind. Crops Prod.* https://doi.org/10.1016/j.indcrop.2014.05.040 (2014).
37. Elenwo, E. I. & Akankali, J. A. The estimation of potential yield of water hyacinth: a tool for environmental management and an economic resource for the Niger Delta Region. *J. Sustain. Dev. Stud.* **9**(2), 115 (2016).
38. G, A., S, B., K, M. P., G, S. & U, G. P. Extraction and molecular characterization of biological compounds from water hyacinth. *J. Med. Plants Stud.* https://doi.org/10.22271/plants.2020.v8.i5a.1189 (2020).
39. Shanab, S. M. M., Shalaby, E. A., Lightfoot, D. A. & El-Shemy, H. A. Allelopathic effects of water hyacinth [*Eichhornia crassipes*]. *PLoS ONE* https://doi.org/10.1371/journal.pone.0013200 (2010).
40. Haggag, M. W., Abou El Ella, S. M. & Abouziena, H. F. Phytochemical analysis, antifungal, antimicrobial activities and application of *Eichhornia crassipes* against some plant pathogens. *Planta Daninha* **35**, e17159560. https://doi.org/10.1590/s0100-83582017350100026 (2017).
41. Aboul-Enein, A. M. et al. *Eichhornia crassipes* (Mart) solms from water parasite to potential medicinal remedy. *Plant Signal. Behav.* https://doi.org/10.4161/psb.6.6.15166 (2011).
42. Shanab, S. M. M., Hanafy, E. A. & Shalaby, E. A. Water hyacinth as non-edible source for biofuel production. *Waste Biomass Valoriz.* https://doi.org/10.1007/s12649-016-9816-6 (2018).
43. Ghaffari-Moghaddam, M., Hadi-Dabanlou, R., Khajeh, M., Rakhshanipour, M. & Shameli, K. Green synthesis of silver nanoparticles using plant extracts. *Korean J. Chem. Eng.* **31**(4), 548–557. https://doi.org/10.1007/s11814-014-0014-6 (2014).
44. Martínez-Espinosa, J. C., Ramírez-Morales, M. A. & Carrera-Cerritos, R. Silver nanoparticles synthesized using *Eichhornia crassipes* extract from Yuriria Lagoon, and the perspective for application as antimicrobial agent. *Crystals* **12**(6), 814. https://doi.org/10.3390/cryst12060814 (2022).
45. Martínez-espinosa, J. C., Ramírez-morales, M. A. & Carrera-cerritos, R. Silver nanoparticles synthesized using *Eichhornia crassipes* extract from Yuriria Lagoon, and the perspective for application as antimicrobial agent. *Crystals* https://doi.org/10.3390/cryst12060814 (2022).
46. Veerasamy, R. et al. Biosynthesis of silver nanoparticles using mangosteen leaf extract and evaluation of their antimicrobial activities. *J. Saudi Chem. Soc.* https://doi.org/10.1016/j.jscs.2010.06.004 (2011).
47. Mochochoko, T., Oluwafemi, O. S., Jumbam, D. N. & Songca, S. P. Green synthesis of silver nanoparticles using cellulose extracted from an aquatic weed; water hyacinth. *Carbohydr. Polym.* https://doi.org/10.1016/j.carbpol.2013.05.038 (2013).
48. Sohail, M., Khurshid, M., Murtaza Saleem, H. G., Javed, H. & Khan, A. A. Characteristics and antibiotic resistance of urinary tract pathogens isolated from Punjab, Pakistan. *Jundishapur J. Microbiol.* **8**(7), e19272. https://doi.org/10.5812/jjm.19272v2 (2015).
49. Ghanbari, F. et al. An epidemiological study on the prevalence and antibiotic resistance patterns of bacteria isolated from urinary tract infections in Central Iran. *Avicenna J. Clin. Microbiol. Infect.* https://doi.org/10.5812/ajcmi.42214 (2017).
50. Jacob Inbaneson, S., Ravikumar, S. & Manikandan, N. Antibacterial potential of silver nanoparticles against isolated urinary tract infectious bacterial pathogens. *Appl. Nanosci.* https://doi.org/10.1007/s13204-011-0031-2 (2011).
51. Kumar, C. G. & Poornachandra, Y. Biodirected synthesis of Miconazole-conjugated bacterial silver nanoparticles and their application as antifungal agents and drug delivery vehicles. *Colloids Surf. B Biointerfaces* https://doi.org/10.1016/j.colsurfb.2014.11.025 (2015).
52. Ahmed, I., Rabbi, M. B. & Sultana, S. Antibiotic resistance in Bangladesh: A systematic review. *Int. J. Infect. Dis.* https://doi.org/10.1016/j.ijid.2018.12.017 (2019).
53. Nadaf, S. J. et al. Green synthesis of gold and silver nanoparticles: Updates on research, patents, and future prospects. *OpenNano* https://doi.org/10.1016/j.onano.2022.100076 (2022).
54. Rasool, U. & Hemalatha, S. Marine endophytic actinomycetes assisted synthesis of copper nanoparticles (CuNPs): Characterization and antibacterial efficacy against human pathogens. *Mater. Lett.* **194**, 176. https://doi.org/10.1016/j.matlet.2017.02.055 (2017).
55. Chowdhury, F. et al. Prevalence of colonization with antibiotic-resistant organisms in hospitalized and community individuals in Bangladesh, a phenotypic analysis: Findings from the antibiotic resistance in communities and hospitals (ARCH) study. *Clin. Infect. Dis.* **77**, 254. https://doi.org/10.1093/cid/ciad254 (2023).
56. Rathod, D., Golinska, P., Wypij, M., Dahm, H. & Rai, M. A new report of *Nocardiopsis valliformis* strain OT1 from alkaline Lonar crater of India and its use in synthesis of silver nanoparticles with special reference to evaluation of antibacterial activity and cytotoxicity. *Med. Microbiol. Immunol.* https://doi.org/10.1007/s00430-016-0462-1 (2016).
57. Bhambure, R., Bule, M., Shaligram, N., Kamat, M. & Singhal, R. Extracellular biosynthesis of gold nanoparticles using *Aspergillus niger* - its characterization and stability. *Chem. Eng. Technol.* https://doi.org/10.1002/ceat.200800647 (2009).
58. Judy, J. D., Tollamadugu, N. V. K. V. P. & Bertsch, P. M. Pin oak (*Quercus palustris*) leaf extract mediated synthesis of triangular, polyhedral and spherical gold nanoparticles. *Adv. Nanoparticles* https://doi.org/10.4236/anp.2012.13011 (2012).
59. Parashar, V., Parashar, R., Sharma, B. & Pandey, A. C. Parthenium leaf extract mediated synthesis of silver nanoparticles: A novel approach towards weed utilization. *Dig. J. Nanomater. Biostruct.* **4**(1), 45 (2009).
60. Mittal, A. K., Chisti, Y. & Banerjee, U. C. Synthesis of metallic nanoparticles using plant extracts. *Biotechnol. Adv.* https://doi.org/10.1016/j.biotechadv.2013.01.003 (2013).
61. Siddiqi, K. S., Husen, A. & Rao, R. A. K. A review on biosynthesis of silver nanoparticles and their biocidal properties. *J. Nanobiotechnol.* https://doi.org/10.1186/s12951-018-0334-5 (2018).
62. Birla, S. S., Gaikwad, S. C., Gade, A. K. & Rai, M. K. Rapid synthesis of silver nanoparticles from *Fusarium oxysporum* by optimizing physicocultural conditions. *Sci. World J.* https://doi.org/10.1155/2013/796018 (2013).

63. Abdulqahar, F. W., Almuhamady, A. K. & Al Taee, M. A. Characterization and antibacterial activity of silver nanoparticles biosynthesized by using aquatic weeds extracts. *Environ. Nanotechnol. Monit. Manag.* https://doi.org/10.1016/j.enmm.2020.100406 (2021).
64. Ullah, I. et al. *Peganum harmala* L. extract-based gold (Au) and silver (Ag) nanoparticles (NPs): Green synthesis, characterization, and assessment of antibacterial and antifungal properties. *Food Sci. Nutr.* https://doi.org/10.1002/fsn3.4112 (2024).
65. Fayaz, A. M. et al. Biogenic synthesis of silver nanoparticles and their synergistic effect with antibiotics: A study against gram-positive and gram-negative bacteria. *Nanomedicine (Lond.)* https://doi.org/10.1016/j.nano.2009.04.006 (2010).
66. Bagherzadeh Homaee, M. & Ehsanpour, A. A. Silver nanoparticles and silver ions: Oxidative stress responses and toxicity in potato (*Solanum tuberosum* L.) grown in vitro. *Hortic. Environ. Biotechnol.* https://doi.org/10.1007/s13580-016-0083-z (2016).
67. Jain, S. & Mehata, M. S. Medicinal plant leaf extract and pure flavonoid mediated green synthesis of silver nanoparticles and their enhanced antibacterial property. *Sci. Rep.* **7**(1), 15867. https://doi.org/10.1038/s41598-017-15724-8 (2017).
68. Janardhanan, R., Karuppaiah, M., Hebalkar, N. & Rao, T. N. Synthesis and surface chemistry of nano silver particles. *Polyhedron* https://doi.org/10.1016/j.poly.2009.05.038 (2009).
69. Raja, S., Ramesh, V. & Thivaharan, V. Green biosynthesis of silver nanoparticles using *Calliandra haematocephala* leaf extract, their antibacterial activity and hydrogen peroxide sensing capability. *Arab. J. Chem.* https://doi.org/10.1016/j.arabjc.2015.06.023 (2017).
70. Bhakya, S., Muthukrishnan, S., Sukumaran, M. & Muthukumar, M. Biogenic synthesis of silver nanoparticles and their antioxidant and antibacterial activity. *Appl. Nanosci. (Switzerland)* https://doi.org/10.1007/s13204-015-0473-z (2016).
71. Dipankar, C. & Murugan, S. The green synthesis, characterization and evaluation of the biological activities of silver nanoparticles synthesized from *Iresine herbstii* leaf aqueous extracts. *Colloids Surf. B Biointerfaces* **98**, 112. https://doi.org/10.1016/j.colsurfb.2012.04.006 (2012).
72. Lokina, S., Stephen, A., Kaviyarasan, V., Arulvasu, C. & Narayanan, V. Cytotoxicity and antimicrobial activities of green synthesized silver nanoparticles. *Eur. J. Med. Chem.* **76**, 10. https://doi.org/10.1016/j.ejmech.2014.02.010 (2014).
73. Roy, N. et al. Biogenic synthesis of Au and Ag nanoparticles by Indian propolis and its constituents. *Colloids Surf. B Biointerfaces* https://doi.org/10.1016/j.colsurfb.2009.11.011 (2010).
74. Rufchaei, R., Abbas-Mohammadi, M., Mirzajani, A. & Nedaei, S. Evaluation of the chemical compounds and antioxidant and antimicrobial activities of the leaves of *Eichhornia crassipes* (Water Hyacinth). *Jundishapur J. Nat. Pharm. Prod.* **17**(1), 101436. https://doi.org/10.5812/jjnpp.101436 (2022).
75. Hamouda, T. et al. A novel surfactant nanoemulsion with a unique non-irritant topical antimicrobial activity against bacteria, enveloped viruses and fungi. *Microbiol. Res.* https://doi.org/10.1078/0944-5013-00069 (2001).
76. Xu, L. et al. Silver nanoparticles: Synthesis, medical applications and biosafety. *Theranostics* https://doi.org/10.7150/thno.45413 (2020).
77. Quinteros, M. A., Cano Aristizábal, V., Dalmasso, P. R., Paraje, M. G. & Páez, P. L. Oxidative stress generation of silver nanoparticles in three bacterial genera and its relationship with the antimicrobial activity. *Toxicol. In Vitro* **36**, 216–223. https://doi.org/10.1016/j.tiv.2016.08.007 (2016).
78. Ali, H. M. et al. Reactive oxygen species induced oxidative damage to DNA, lipids, and proteins of antibiotic-resistant bacteria by plant-based silver nanoparticles. *3 Biotech* **13**(12), 414. https://doi.org/10.1007/s13205-023-03835-1 (2023).
79. Xu, H. et al. Role of reactive oxygen species in the antibacterial mechanism of silver nanoparticles on *Escherichia coli* O157:H7. *Biometals* **25**(1), 45–53. https://doi.org/10.1007/s10534-011-9482-x (2012).
80. Lakkim, V. et al. Green synthesis of silver nanoparticles and evaluation of their antibacterial activity against multidrug-resistant bacteria and wound healing efficacy using a murine model. *Antibiotics* **9**(12), 902. https://doi.org/10.3390/antibiotics9120902 (2020).
81. Gandhi, H. & Khan, S. Biological synthesis of silver nanoparticles and its antibacterial activity. *J. Nanomed. Nanotechnol.* **07**(02), 1000366. https://doi.org/10.4172/2157-7439.1000366 (2016).
82. Silva, L. P., Silveira, A. P., Bonatto, C. C., Reis, I. G. & Milreu, P. V. Silver nanoparticles as antimicrobial agents. In *Nanostructures for antimicrobial therapy* 577–596 (Elsevier, Amsterdam, 2017). https://doi.org/10.1016/B978-0-323-46152-8.00026-3.
83. Dragieva, I., Stoeva, S., Stoimenov, P., Pavlikianov, E. & Klabunde, K. Complex formation in solutions for chemical synthesis of nanoscaled particles prepared by borohydride reduction process. *Nanostruct. Mater.* **12**(1–4), 267–270. https://doi.org/10.1016/S0965-9773(99)00114-2 (1999).
84. Marsh, P. D. Controlling the oral biofilm with antimicrobials. *J. Dent.* https://doi.org/10.1016/S0300-5712(10)70005-1 (2010).
85. Garibo, D. et al. Green synthesis of silver nanoparticles using *Lysiloma acapulcensis* exhibit high-antimicrobial activity. *Sci. Rep.* https://doi.org/10.1038/s41598-020-69606-7 (2020).
86. Abu-Tahon, M. A., Ghareib, M. & Abdallah, W. E. Environmentally benign rapid biosynthesis of extracellular gold nanoparticles using *Aspergillus flavus* and their cytotoxic and catalytic activities. *Process Biochem.* https://doi.org/10.1016/j.procbio.2020.04.015 (2020).
87. Aljabali, A. A. A. et al. Synthesis of gold nanoparticles using leaf extract of *ziziphus zizyphus* and their antimicrobial activity. *Nanomaterials* https://doi.org/10.3390/nano8030174 (2018).

Acknowledgements

We express our gratitude to the Department of Biotechnology and Genetic Engineering at Gopalganj Science and Technology University for funding this research and Islamic University for their assistance with SPR and UV-vis spectroscopy, as well as to the Kushtia Sadar Hospital Authority for their support in sample collection. Special thanks to Khulna Agricultural University, Bangladesh and Patuakhali Science and Technology University, Bangladesh, for support and help. The authors were also supported by funding from the Gopalganj Science and Technology University Research Cell (gstu534524).

Author contributions

Imdadul Haque Sharif: Conceptualization, Writing—original draft, Investigation, Methodology, Formal analysis. Farjana Sultana Primu: Writing—original draft, Investigation, Formal analysis. Md. Nahid Hasan Joy: Writing—original draft, Formal analysis, Methodology, Investigation. Monika Halder Tithi: Writing—original draft, Investigation, Methodology. Ashik Chowdhury: Writing—original draft, Formal analysis, reviewing, & Validation. Pradipta Debnath Pretha: Conceptualization, Writing—original draft, Investigation, Validation, Methodology. Abu Hena Mostafa Jamal: Writing—original draft, Investigation, Methodology, Formal analysis, Supervision. Tusar Kanti Roy: Writing—original draft, Methodology, Formal analysis. Zulhilmi Ismail: Writing—reviewing and editing. Md. Saiful Islam: Writing—original draft, Formal analysis, Supervision, Resources. Abubakr M. Idris: Writing—review & editing, Validation, Supervision, Resources.

Funding
The authors extend their appreciation to the Deanship of Research and Graduate Studies at King Khalid University, KSA, for funding this work through the Small Research Group under grant number (RGP.1/266/46).

Competing interests
The authors declare no competing interests.

Ethical approval
This study was conducted in compliance with ethical standards and guidelines. The study did not involve the use of any animal models or human participants. In the current study, Ag NPs via plant-derived material and their antibacterial and antifungal efficacy against bacterial and fungal species were assessed. All experimental procedures were carried out according to institutional and international ethical standards for laboratory-based research.

Consent for publication
All of the authors have read and approved the paper, and it has not been published previously nor is it being considered by any other peer-reviewed journal. Also, this manuscript has not been submitted to any preprint server before submission.

Compliance with ethical standards
The authors declare no conflicts of interest, and ethical approval, consent to participate, and data-availability statements do not apply to this study.

Additional information
Supplementary Information The online version contains supplementary material available at https://doi.org/10.1038/s41598-026-41224-9.

Correspondence and requests for materials should be addressed to T.K.R., Z.I., M.S.I. or A.M.I.